Three-Dimensional Monte Carlo Simulation of Grain Growth in Zone-Refined Iron

S. SISTA and T. DEBROY

The evolution of the grain structure and topological-class distributions in zone-refined iron were modeled using a three-dimensional (3-D) Monte Carlo (MC) model. The effect of grain size on topological features was examined. The relationship between the topological features of grains and the geometry of their surrounding grains was studied. In particular, the average number of sides of the grains was related to the average number of sides of their neighbors. Both the computed grain-size distribution and the topological-class distribution were found to be invariant with time. A linear relationship existed between the average grain size and the average number of sides of grains. The number of sides of grains was inversely proportional to the average number of sides of the neighboring grains. The computed average grain size, grain-size distribution, and topological-class distribution agreed well with the corresponding independent experimental data. The results indicate significant promise for understanding grain growth and topological features using 3-D MC simulation.

I. INTRODUCTION

GRAIN-SIZE changes during processing of metals and alloys may affect their strength, toughness, ductility, and corrosion resistance.[1] As a result, the prediction and control of grain-structure evolution have received considerable attention. Analytical models have been developed to understand the effects of time and temperature on the grain-size changes. These models often describe grain growth by the following parabolic equation, derived by considering growth due to the change in grain-boundary energy.[2–6]

$$L^n = Ct \qquad [1]$$

where L is the average grain size; n is the grain-growth exponent, which was derived[2–6] as 2.0; C is a temperature-dependent parameter; and t is time. However, measurements[7] on various metallic systems have shown that the grain-growth exponent may be more than 2.0 in many cases.

The discrepancy between the experimental data[7,8] and the results from analytical models[2–6] can be attributed to the simplifying assumptions inherent in the models. The most common assumption of a spherical grain shape leads to an unrealistic estimation of the grain surface area and violates the fundamental topological mandate to share interfacial planes between neighboring grains in a dense crystalline solid. Furthermore, the previous analytical models considered growth of isolated grains which were unaffected by the neighboring grains in the matrix. A rigorous analytical treatment of grain growth, considering all its component physical processes and topological constraints, is not yet available.

With the development of computational techniques in the last two decades that take into account both the grain-growth kinetics and the topological features, some of the common assumptions in the analytical models have been relaxed. As a result, more-realistic calculations of grain growth have become possible. Among the computational models, Monte Carlo (MC) simulation[7,8,10–22] has been widely used to simulate grain growth under both isothermal and nonisothermal conditions. Most of the calculations reported in the literature have been performed in two dimensions.[7,8,10–12,16,17] A few notable exceptions include some recent works, where calculations were done in three dimensions.[8,14,15,20–22]

There are considerable computational challenges in conducting meaningful MC calculations. The main difficulty is in the processing of a large volume of data in a realistic time frame. For example, the simulation in a 100×100 two-dimensional grid, considering 200 MC simulation steps, involves 2.0 million ($100 \times 100 \times 200$) data points per variable. For a more realistic simulation, a three dimensional (3-D) calculation with $100 \times 100 \times 100$ grid points undergoing 200 iteration steps will increase the number of data points to 200 million per variable. This two-order-of-magnitude increase in the volume of data presents several interesting challenges even for the most powerful modern computers. Only in recent years have such large-scale computations become tractable, because of advances in the computational hardware. Furthermore, modern data visualization techniques and tools have to be pushed to their limits just to visualize the computed results, even in an efficient binary format.

Grain growth and topological features of grains have received considerable attention in the literature[3–15,26–29] for various reasons. Grain surfaces and edges provide heterogeneous nucleation sites for important reactions. A relation between the average grain size and grain shape (number of sides) is important, because grain growth is influenced by both kinetic and topological factors. Grains with a large number of sides (lower grain-boundary length per unit area) are energetically favored to grow at the expense of their neighboring grains.[9] Growth of a grain should always be examined by considering its relation to its neighbors, since grains do not grow in isolation. Therefore, it is important to know the relationship between the shape of the neighboring grains and the shape of the grains they surround.

S. SISTA, formerly Graduate Student, Department of Materials Science and Engineering, The Pennsylvania State University, is Computer Aided Design Engineer, Intel Corporation, Hillsboro, OR 97124. T. DEBROY, Professor, is with the Department of Materials Science and Engineering, The Pennsylvania State University, University Park, PA 16802.

Manuscript submitted November 14, 2000.

There are important differences between the research presented in this article and in previous works[8,14,15,20–22] that addressed grain growth in three dimensions. The differences lie in the implementation of the basic MC algorithm and in the analysis of the results. References 8 and 14 consider all possible interactions in the system, involving all grid points for the changing orientation of a location during the reorientation step. However, in calculations with large grids, this approach is time consuming and unnecessary in many cases, as grain-boundary migration involves atomic jumps toward nearest-neighbor sites in adjacent grains.[13] In the current work, only the nearest-neighbor grid points are considered in the reorientation step. Our previous research[20,21,22] addressed grain growth under nonisothermal conditions. However, the topology of the grains was not investigated. In contrast, References 8, 14, and 15 addressed the topology of grains. However, these publications did not investigate either the relation between the grain-size distribution and topological-class distribution or the decrease in grain perimeter with time.

Although there is a growing body of literature on the algorithms to compute grain growth, the application of these algorithms to simulate grain growth in real materials has not received much attention. Here, we report a comprehensive effort to develop a 3D MC simulation model for grain growth by considering both the grain-growth kinetics and topological features in zone-refined iron. This article analyzes the grain growth, decrease in the net grain perimeter per unit area, grain-size distribution, and topological-class distribution. The interrelationships between these properties are also examined. The MC model predictions are compared with independent experimental results.[9]

II. MATHEMATICAL MODELING

A. *Monte Carlo Simulation of Grain Growth*

The application of the MC technique to simulate grain growth has been described in detail in the literature.[1,7–17] Only the salient features of this technique are described here. Each grid point is assigned a random orientation number between 1 and q, where q is the total number of grain orientations. The value of q was taken to be 48 in the present simulation, since it is known that the grain-growth exponent becomes almost independent of q when its value is larger[7] than 30. Two adjacent grid points having the same orientation number are considered to be a part of the same grain; otherwise, they belong to different grains. The grain-boundary energy is specified by defining an interaction between nearest-neighbor lattice sites. The local interaction energy (E) is calculated by the Hamiltonian equation:

$$E = -J \sum_{j=1}^{n} (\delta_{S_i S_j} - 1) \qquad [2]$$

where J is a positive constant which sets the scale of the grain-boundary energy, δ is the Kronecker's delta function, S_i is the orientation at a randomly selected site i, S_j is the orientation of its nearest neighbor, and n is the total number of the nearest-neighbor sites. Each pair of nearest neighbors contributes J to the system energy when they are of unlike orientation and zero otherwise. The Kronecker's delta function in Eq. [2] is defined as

$$\delta_{S_i S_j} = 1 \quad \text{when} \quad S_i = S_j \qquad [3]$$

$$\delta_{S_i S_j} = 0 \quad \text{when} \quad S_i \neq S_j \qquad [4]$$

The kinetics of grain-boundary migration are simulated by selecting a site randomly and changing its orientation to one of the nearest-neighbor orientations based on the energy change due to the attempted orientation change. The probability of the orientation change is defined as

$$p = 1 \quad \text{for} \quad \Delta E \leq 0 \qquad [5]$$

$$p = e^{\frac{-\Delta E}{k_B T}} \quad \text{for} \quad \Delta E > 0 \qquad [6]$$

where ΔE is the change of energy due to the change of orientation, k_B is the Boltzman constant, and T is the absolute temperature. A successful transition at the grain boundaries to orientations of nearest-neighbor grains corresponds to boundary migration.

In a 3-D simulation, the total number of the nearest first, second, and third neighbors[15,20–22] is 26. The energy difference due to attempted orientation switching is calculated by

$$\Delta E = J \sum_{i=1}^{26} (\delta_{S_i S_0} - \delta_{S_i S_n}) \qquad [7]$$

where S_0 is the original orientation number, S_i represents the orientation numbers of its nearest neighbors, and S_n is a new orientation number. It should be noted that the grain-boundary energy is treated as isotropic in Eqs. [2] and [7].

B. *Isothermal Grain-Growth Kinetics from MC Simulations*

Through the MC simulation, an empirical relation[16] between the simulated grain size and the MC simulation time can be obtained as

$$L = K_1 \lambda (t_{\mathrm{MCS}})^{n_1} \qquad [8]$$

where L is the simulated average grain size measured by average grain intercepts, λ is the discrete grid-point spacing in the MC technique, t_{MCS} is the MC simulation time, and K_1 and n_1 are the model constants, which are obtained by regression analysis of the data generated from the MC simulation. It should be noted that the MC simulation time (t_{MCS}) in Eq. [8] is a dimensionless quantity.

An experimental data–based (EDB) kinetic model proposed by Gao and Thompson[16] was used to relate t_{MCS} to real time because of the availability of experimental data.[9] According to the EDB model, the following relation can be obtained, by multiple regression analysis of the isothermal experimental data, between the average grain size (L), average initial grain size (L_o), holding time (t), and temperature (T):

$$L^n - L_0^n = Kte^{\left(\frac{Q}{RT}\right)} \qquad [9]$$

where K is a constant and Q is the activation energy. Both K and Q are obtained from experimental data[23] and are given in Table I. Hu[9] noted that the value of n in Eq. [9] changes with temperature. At the temperature considered in this study (923 K), n is about 2.7 for zone-refined iron. This result was obtained by neglecting the initial average grain size and the sample thickness. Vandermeer and Hu[23] later represented grain growth in terms of a single, thermally

Table I. Computational and Material Parameters Used in the Calculations for Zone-Refined Iron

Parameter	Value	Reference
Grid spacing, λ (μm)	40	—
Total number of grain orientations, q	48	—
Initial average grain size, L_0 (μm)	40	23
Number of iteration steps	200	—
Temperature (K)	923	9
Simulation constant, K_1	1.01	—
Simulation constant, n_1	0.42	—
Experimental grain growth exponent, n	2.0	23
Activation energy (kJ/mol)	250	9
Pre-exponential factor, K (m^2/s)	528	23

activated rate process by considering both the initial average grain size and sample thickness and arrived at a constant value of $n = 2.0$ over the entire temperature range (823 to 1123 K) considered in the experiments of Hu.[9] The same value of the experimental grain-growth exponent, $n = 2.0$, is considered here.

Substituting Eq. [8] into [9], a relationship between the MC simulation time and real time and temperature is obtained:

$$(t_{MCS})^{nn_1} = \left(\frac{L_0}{K_1\lambda}\right)^n + \frac{Kt}{(K_1\lambda)^n} e^{-\frac{Q}{RT}} \qquad [10]$$

In the present investigation, 3-D simulations were carried out in a simple cubic 100 × 100 × 100 grid with a grid spacing[9] of 40 μm. The computational and material parameters used for the calculation are provided in Table I.

Topological attributes and the average grain size were determined in the following six planes: $X = 1.32$ mm, $Y = 1.32$ mm, $Z = 1.32$ mm, $X = 2.64$ mm, $Y = 2.64$ mm, and $Z = 2.64$ mm in the 4 × 4 × 4 mm domain. The lineal-intercept method[24] was used in the calculation of average grain size. Since the MC simulation results can vary from run to run, the grain-growth and topological results presented in this article are averaged over five runs to examine this variation. The run-to-run variations of the results are indicated by error bars in the figures.

III. RESULTS AND DISCUSSION

The calculated average grain sizes as a function of t_{MCS} for all five runs are shown in Figure 1. The variation of the average grain size ranged from ±2.1 pct at low values of t_{MCS} (<40) to ±3.0 pct at high values of t_{MCS} (>160). The evolution of simulated grain structure and the continuous increase in the average grain size with time are shown in Figure 2.

The calculated values of average grain size and the grain perimeter as a function of time are shown in logarithmic scales in Figure 3. It is observed that the calculated and the experimentally measured values[9] are comparable. Except at very short times (<2000 seconds), the average grain-size data in Figure 3 can be represented by Eq. [1]. In the initial period, L_0 in Eq. [9] cannot be neglected, and the computed results do not fit Eq. [1]. After the initial period, the total length of the grain boundary per unit area, *i.e.*, the grain perimeter per unit area, decreases with time at the same rate as the rate of increase in the average grain size. The radius

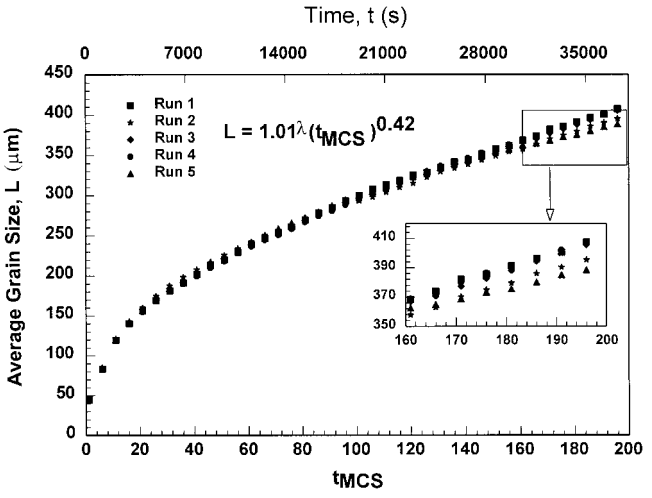

Fig. 1—Calculated average grain size as a function of MC simulation time, t_{MCS}, for five runs. A section of the plot is magnified for clarity. The symbol λ represents grid spacing, which is taken as 40 μm in the present article.

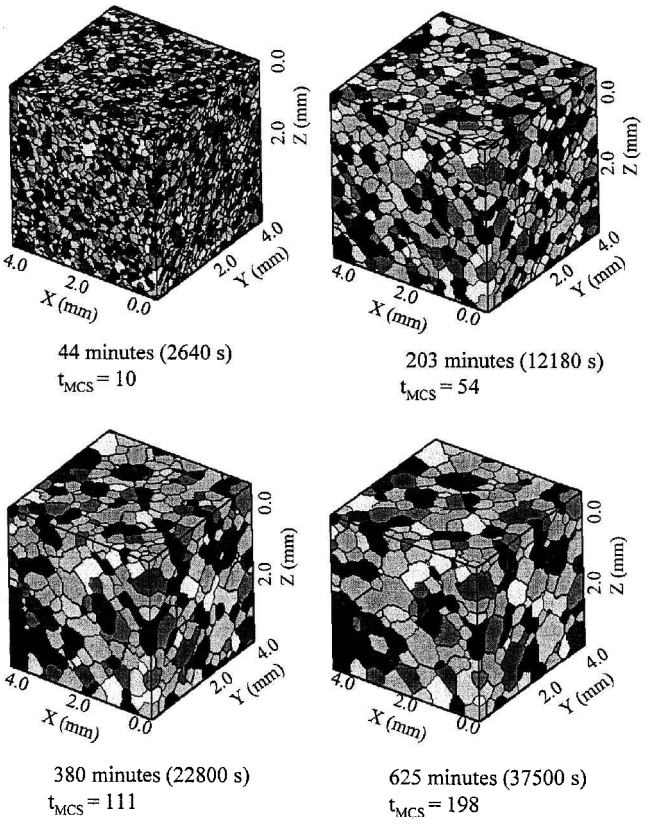

Fig. 2—Evolution of 3-D-simulated grain structure with a 100 × 100 × 100 grid system as a function of time.

of curvature of a grain boundary is inversely proportional to the perimeter per unit area[10] and directly proportional to the average grain size. Thus, an increase in the logarithm of average grain size is accompanied by a decrease in the logarithm of net grain perimeter per unit area, making the two rates almost the same in magnitude.

Figures 4(a) and (b) show the grain-size distribution at 125 and 625 minutes (7500 and 37500 seconds), respectively. The frequency values represent the ratio of the number

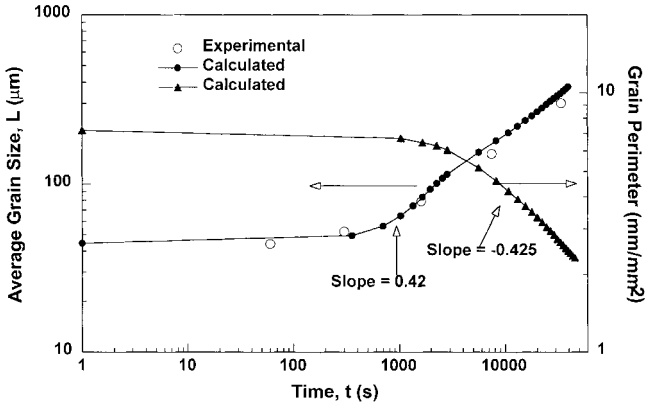

Fig. 3—Calculated and experimentally determined[9] average grain size and the computed grain perimeter as a function of time.

of grains with R/R_{avg} values in any chosen interval of 0.2 and the total number of grains. The grain-size distributions from both simulations and experiments exhibit asymmetric peaks in the range of R/R_{avg} between 0.5 and 1.5. The largest grains are about 2.5 to 3.5 times the average grain size. The computed average grain-size distributions are compared with the experimental data reported by Hu[9] in Figure 4(c). It can be observed that the frequency-distribution curves did not change with time, as has been observed by Hu.[9] Furthermore, the computed values agreed well with the experimental results. The computed grain-size distributions are also compared with the corresponding analytically calculated distributions proposed by Feltham[5] and Louat[6] in Figure 4(c). It is instructive to review, very briefly, the salient features of the calculations. Both authors adopted a "mean-field approach," according to which the overall flux, j, is given by[25]

$$j = -D\frac{\partial f}{\partial R} + fv \qquad [11]$$

where D can be identified with a diffusion coefficient that depends on the specific grain-boundary mobility, and f is the distribution function, which is affected by both grain size (R) and time. The first term in the right-hand side represents a diffusion-like process,[25] in which grains larger than R_{avg} grow due to a "concentration gradient" ($\partial f/\partial R$), and the second term refers to a drift velocity (v) which originates due to the reduction in grain-boundary area. The physical basis for the diffusion-like process is not clear and has been questioned in the literature.[8,25]

Feltham[5] assumed that the drift term in Eq. [11] dominates normal grain growth. He derived the following expression for the velocity, assuming f to have a log-normal distribution:

$$v = \frac{K}{R}\ln\left(\frac{R}{R_{avg}}\right) \qquad [12]$$

where K is a constant used previously in Eq. [9]. Equation [12] may be rewritten as

$$\frac{dR^2}{dt} = 2K\ln\left(\frac{R}{R_{avg}}\right) \qquad [13]$$

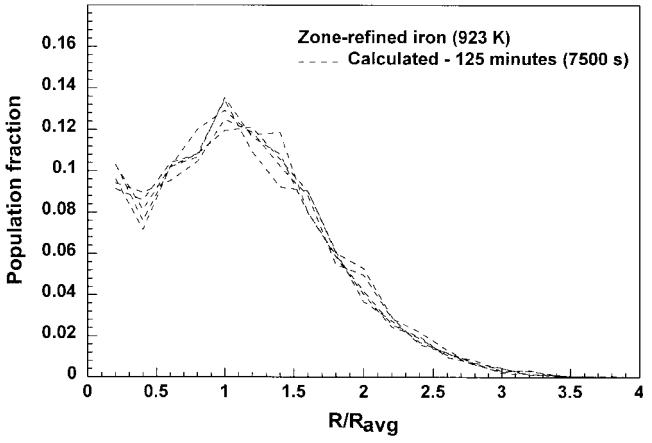

(*a*)

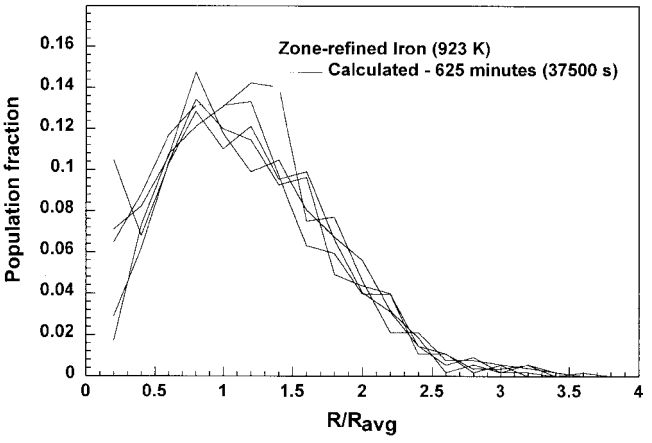

(*b*)

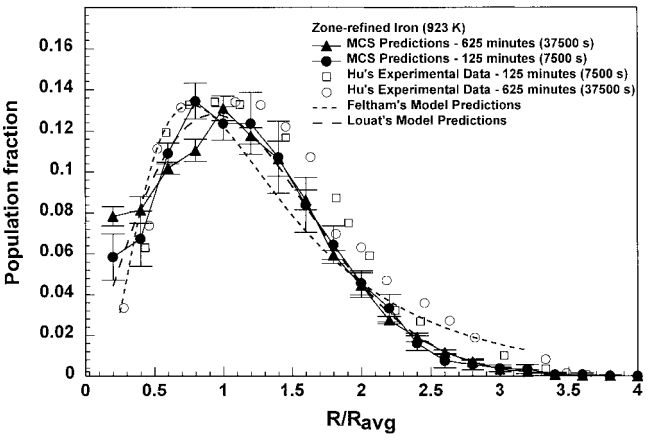

(*c*)

Fig. 4—(*a*) and (*b*) The grain size distribution shown for five runs at 125 min (7500 s) and 625 min (37,500 s). (*c*) The grain size distribution as an average of five runs from the present simulation compared with Hu's[9] data for zone-refined iron and the theoretical distributions of Feltham[5] and Louat.[6]

Setting $R = R_{max} = 2.5R_{avg}$ from experimental data and assuming the log-normal distribution to be time invariant, he obtained parabolic growth kinetics. The following expression for f was considered by Feltham:[5]

$$f = \frac{b_1}{b_2\pi^{1/2}}\,e^{-\frac{2\left(\ln\left(\frac{R}{R_{avg}}\right)-b_3\right)^2}{b_2^2}} \qquad [14]$$

Table II. Computed Values of the Constants in Equations [14] and [17]

Constant	Value	Standard Error	Standard Deviation	Confidence
b_1	0.31	0.66×10^{-1}		
b_2	1.32	0.11	0.48×10^{-1}	92 pct
b_3	0.27	0.26×10^{-1}		
β	0.23	0.89×10^{-2}		
α	0.57	0.23×10^{-1}	0.48×10^{-1}	96 pct

where b_1, b_2, and b_3 are constants. The values of these constants were obtained by least-squares fitting of Eq. [14] to the calculated 3-D MC results reported in this article. The values of these constants, their standard errors, the standard deviation of f, and the confidence level of f are presented in Table II.

Louat,[6] on the other hand, argued that the boundary motion is a random process and considered only the diffusion term in Eq. [11] to solve for the grain-size distribution. Assuming D to be independent of R and the distribution to be time invariant, he obtained the following expression for the grain-size distribution:

$$f = \frac{C_5 R e^{-\frac{R^2}{4Dt}}}{Dt^{3/2}} \qquad [15]$$

where C_5 is a constant. The value of R_{avg} considered by Louat[6] is given by

$$R_{avg} = \sqrt{2\pi Dt} \qquad [16]$$

Combining Eq. [15] and [16], the following expression for f is obtained:

$$f = \beta \frac{R}{R_{avg}} e^{-\alpha\left(\frac{R}{R_{avg}}\right)^2} \qquad [17]$$

where β and α are constants. The values of these constants were obtained by least-squares fitting of the 3-D MC simulation results in Eq. [17]. The values of these constants, their standard errors, the standard deviation of f, and the confidence level of f are presented in Table II.

From Figure 4(c), it can be observed that the Louat's[6] distribution appears to give a slightly better fit to the calculated MC results than Feltham's[5] log-normal distribution. Anderson *et al.*[8] attributed the difference between their results to the fact that Feltham assumed spherical grains, whereas Louat considered polygonal grains. Even though Louat's distribution gives a good fit, the mean-field theories of both Feltham and Louat neglected the effect of neighboring grains. Furthermore, topological considerations were ignored in these theories.

Figure 5 shows the grain-size distribution frequency as a function of average grain size for 125, 420, and 625 minutes (7500, 25200, and 37,500 seconds). Two interesting points may be noted from Figure 5. First, the position of the peaks shifts toward higher average grain sizes with time, even though the height of the peaks remains almost the same. Second, the frequency of smaller grains decreases with time, because the larger grains grow with time at the expense of smaller grains.

Figure 6 shows the frequency distribution of the number of grain edges, also called the topological-class distribution.

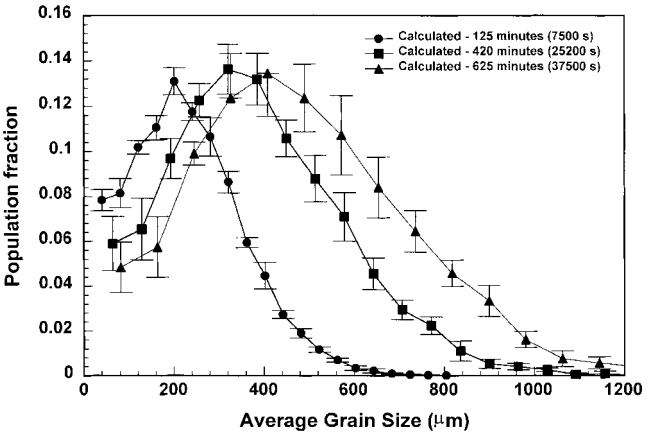

Fig. 5—The grain size distribution as an average of five runs from the present simulation for various times.

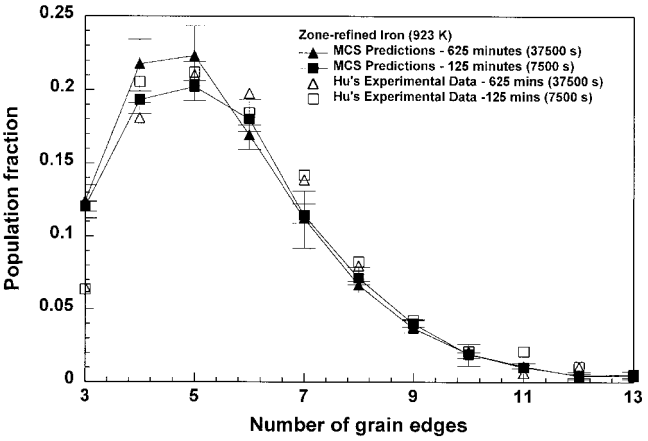

Fig. 6—The distribution of number of sides of a grain from the present simulation compared with Hu's[9] data for zone-refined iron.

It can be observed that the calculated results are comparable with the experimental data.[9] It is also found that the peak frequency of occurrence corresponds to the grains with five edges, although many grains with more than five edges exist. The frequency increases rapidly for a small number of grain edges and decreases when the number of edges exceeds six. The calculated average edges per grain is found to be approximately equal to six. This number is consistent with the general topological rule,[26] which has also been theoretically derived by Mullins[27] and Neumann.[28] Based on the behavior of individual grains and the uniform-boundary model, they obtained a correlation between grain-growth kinetics and the topological class of individual grains:[4]

$$\frac{dR}{dt} = \frac{M\gamma}{R}\left(\frac{n}{6} - 1\right) \qquad [18]$$

where M is the mobility of the grain boundary, γ is the grain-boundary energy, and n is the average number of grain edges. To conserve the total area, the sum of $R \cdot dR/dt$ over all the grains must be zero. Thus, according to Eq. [18], the average number of edges should be six. Therefore, grains with less than six edges will shrink, and grains with more than six edges will grow.

The shape of the topological-class distribution curve in

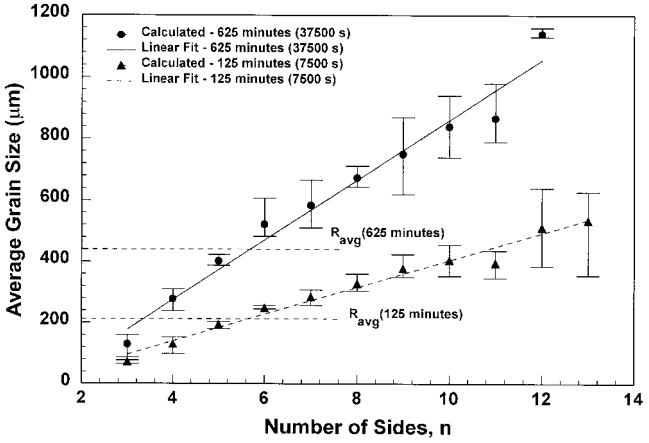

Fig. 7—The average grain size as a function of number of sides of a grain, n, for 125 min (7500 s) and 625 min (37,500 s) at 923 K for the plane Z = 2.64 mm. Also represented are the average grain sizes (R_{avg}) for 125 min (7500 s) and 625 min (37,500 s) taken from Fig. 3.

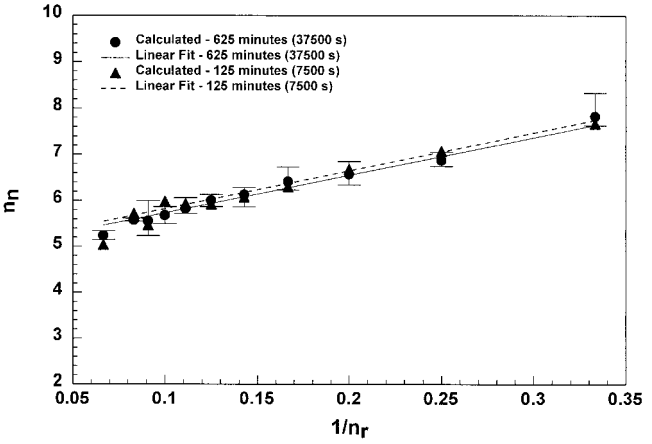

Fig. 8—Average number of sides of neighboring grains, n_n, as a function of the inverse of number of sides, $1/n_r$, for 125 and 625 min (7500 and 37,500 s) at 923 K for the Z = 2.64-mm plane.

Figure 6 is essentially similar to the grain-size distribution plot in Figure 4(c), suggesting that the average number of sides per grain and the grain size may be related. Figure 7 shows linear relationships when the grain size is plotted as a function of the average number of sides per grain. A similar linear relation was observed by Feltham[5] for annealed tin. The horizontal dashed lines in the figure indicate the calculated average grain size for the two times taken from Figure 3. It can be seen that the average grain size corresponds to grains with six sides.

In order to examine the effect of the geometry of the neighboring grains on grain topology, a plot of the average number of sides of neighboring grains (n_n) and the inverse of the number of sides of grains ($1/n_r$) is presented in Figure 8. The values on the Y-axis are the average of the distribution for each topological class. Linear relations of the following form were obtained by a linear least-squares fit to the data averaged from five runs.

$$n_n = H_1 + \frac{H_2}{n_r} \qquad [19]$$

where the values of H_1 and H_2 are 4.92 and 8.16, respectively, after 625 minutes (37,500 seconds). The values of H_1 and H_2 were found to be 5.00 and 8.24 after 125 minutes (7500 seconds). These values are in good agreement with both Hu[8] (H_1 = 5.00 and H_2 = 7.60) and Aboav[29] (H_1 = 5.00 and H_2 = 8.00) for zone-refined iron and magnesium oxide, respectively. Saito and Enomoto[11] also found a similar relation for two-dimensional MC simulations. The significance of the plots in Figure 8 is that they set an important topological rule for the neighboring grains. Since the value of n_r cannot be less than 3, the value of n_n remains in the range of $H_1 + H_2/3$ to H_1. Using the values of H_1 and H_2 from the 3D MC simulation results, the average number of sides of the surrounding grains ranges between 5 and 8.

IV. CONCLUSIONS

A 3-D MC simulation was performed to study the evolution of grain structure in zone-refined iron. It was found that the logarithm of the average grain size increased linearly with the logarithm of time, except at very short times (<2000 seconds). The rate of increase of the average grain size was almost the same as the rate of decrease of the net grain perimeter.

Both the calculated grain-size distribution and topological-class distributions did not change with time. The maximum grain size was about 2.5 to 3.5 times the average size. The topological-class distribution function exhibited a peak when the grains had five edges, indicating that most grains were five sided. The average number of edges per grain was found to be six, which is consistent with theoretical predictions. The average number of sides of the neighboring grains ranged between five and eight. A linear relationship was found between the average grain size and the average number of sides of grains. The experimental grain sizes, grain-size distributions, and topological-class distributions[9] agreed well with the simulated results. The agreement between the calculated and independent experimental[9] results indicated significant promise for understanding grain growth from 3-D MC calculations.

ACKNOWLEDGMENT

This research was supported by a grant from the United States Department of Energy, Office of Basic Energy Sciences, Division of Materials Sciences, under Grant No. DE-FGO2-84ER45158.

REFERENCES

1. S. Ling and M.P. Anderson: *JOM*, 1992, vol. 9, pp. 30-36.
2. J.E. Burke and D. Turnbull: *Prog. Met. Phys.*, 1952, vol. 3, pp. 220-92.
3. S.K. Kurtz and F.M.A. Carpay: *J. Appl. Phys.*, 1980, vol. 51, pp. 5725-44.
4. M. Hillert: *Acta Metall.*, 1965, vol. 22, pp. 227-38.
5. P. Feltham: *Acta Metall.*, 1957, vol. 5, pp. 97-105.
6. N.P. Louat: *Acta Metall.*, 1974, vol. 22, pp. 721-24.
7. M.P. Anderson, D.J. Srolovitz, G.S. Grest, and P.S. Sahni: *Acta Metall.*, 1984, vol. 32, pp. 783-91.
8. M.P. Anderson, G.S. Grest, and D.J. Srolovitz: *Phil. Mag. B*, 1989, vol. 59, pp. 293-329.

9. H. Hu: *Can. Metall. Q.*, 1974, vol. 13, pp. 275-86.
10. D.J. Srolovitz, M.P. Anderson, P.S. Sahni, and G.S. Grest: *Acta Metall.*, 1984, vol. 32, pp. 793-802.
11. Y. Saito and M. Enomoto: *Iron Steel Inst. Jpn. Int.*, 1992, vol. 32, pp. 267-74.
12. G.S. Grest, D.J. Srolovitz, and M.P. Anderson: *Acta Metall.*, 1985, vol. 33 (3), pp. 509-20.
13. B. Radhakrishnan and T. Zacharia: *Metall. Mater. Trans. A*, 1995, vol. 26A, pp. 167-80.
14. M.P. Anderson, G.S. Grest, and D.J. Srolovitz: *Scripta Metall.*, 1985, vol. 19, pp. 225-30.
15. Y. Saito: *Iron Steel Inst. Jpn. Int.*, 1998, vol. 38, pp. 559-66.
16. J. Gao and R.G. Thompson: *Acta Metall.*, 1996, vol. 44, pp. 4565-70.
17. J. Gao, R.G. Thompson, and Y. Cao: in *Trends in Welding Research*, H.B. Smartt, J.A. Johnson, and S.A. David, eds., ASM INTERNATIONAL, Materials Park, OH, 1996, pp. 199-204.
18. B. Radhakrishnan and T. Zacharia: *Metall. Mater. Trans. A*, 1995, vol. 26A, pp. 2123-30.
19. A.L. Wilson, R.P. Martukanitz, and P.R. Howell: in *Trends in Welding Research*, J.M. Vitek, S.A. David, J.A. Johnson, H.B. Smartt, and T. DebRoy, eds., ASM INTERNATIONAL, Materials Park OH, 1999, pp. 161-66.
20. Z. Yang, J.W. Elmer, J. Wong, and T. DebRoy: *Weld. J. Res. Suppl.*, 2000, vol. 79 (4), pp. 97s-112s.
21. Z. Yang, S. Sista, J.W. Elmer, and T. DebRoy: *Acta Mater.*, 2000, vol. 48 (20), pp. 4813-25.
22. S. Sista, Z. Yang, and T. DebRoy: *Metall. Mater. Trans. B*, 2000, vol. 31B, pp. 529-36.
23. R.A. Vandermeer and H. Hu: *Acta Metall. Mater.*, 1994, vol. 42, pp. 3071-75.
24. *Annual Book of ASTM Standards.*, ASTM, West Conshohoken, PA, 1996, vol. 1, Sect. 3.
25. H.V. Atkinson: *Acta Metall.*, 1988, vol. 36, pp. 469-91.
26. C.S. Smith: *Metal Interfaces*, ASM INTERNATIONAL, Materials Park, OH, 1952, pp. 65-108.
27. W.W. Mullins: *J. Appl. Phys.*, 1956, vol. 27, pp. 900-04.
28. J. von Neumann: *Metal Interfaces*, ASM INTERNATIONAL, Materials Park, OH, 1952, pp. 108-11.
29. D.A. Aboav: *Metallography*, 1970, vol. 3, pp. 383-90.